*Article*

# Blade Crack Diagnosis Based on Blade Tip Timing and Convolution Neural Networks

**Guangya Zhu** [1], **Chongyu Wang** [1], **Wei Zhao** [2], **Yonghui Xie** [2], **Ding Guo** [1] **and Di Zhang** [1,*]

[1] MOE Key Laboratory of Thermo-Fluid Science and Engineering, Xi'an Jiaotong University, Xi'an 710049, China
[2] School of Energy and Power Engineering, Xi'an Jiaotong University, Xi'an 710049, China
[*] Correspondence: zhang_di@mail.xjtu.edu.cn; Tel.: +86-13636800216

**Abstract:** The diagnosis of blade crack faults is critical to ensuring the safety of turbomachinery. Blade tip timing (BTT) is a non-contact vibration displacement measurement technique, which has been extensively studied for blade vibration condition monitoring recently. The fault diagnosis methods based on deep learning can be summarized as studying the internal logical relationship of data, automatically mining features, and intelligently identifying faults. This research proposes a crack fault diagnostic method based on BTT measurement data and convolutional neural networks (CNNs) for the crack fault detection of blades. There are two main aspects: the numerical analysis of the rotating blade crack fault diagnosis and the experimental research in rotating blade crack fault diagnosis. The results show that the method outperforms many other traditional machine learning models in both numerical models and tests for diagnosing the depth and location of blade cracks. The findings of this study contribute to the real-time online crack fault diagnosis of blades.

**Keywords:** blade tip timing; blade crack faults; deep learning; fault diagnosis; experimental measurement

## 1. Introduction

Turbomachine blades are subjected to centrifugal force, airflow excitation, and thermal stress when working in high-temperature, high-pressure, and corrosive environments. Therefore, it is easy for cracks, wear, corrosion, and other risks to develop on the blades, which would hasten high-cycle fatigue failure or potential fracture, shorten the service life, and endanger the safety and operational stability of the turbine [1]. The aircraft compressor blade of China Southern Airlines flight CZ3739 cracked in 2014, causing the engine to catch fire in the air. An engine explosion on a United Boeing 777 happened in February 2021, caused by the fatigue fracture of two fan blades of the PW4000 engine, which damaged the magazine and caused the explosion. According to statistics, blade damage caused 70% of forced-stop accidents in turbines in the United States until 2008 [2].

There are many ways to monitor the real-time status of blade crack faults. Spitas et al. [3] measured the change in potential difference by placing three electrodes on the specimen's surface to obtain the shape parameters of the crack. However, this method required attaching electrodes to the surface of the specimen, and the measurement in the rotating state was not independently verified. Krause et al. [4] detected damage to wind turbine rotor blades by using audio classification techniques, but the technique was ineffective for monitoring blades with progressive cracks or in a cabinet with loud airflow. Abouhnik et al. [5] proposed the empirical decomposition characteristic strength level (EDFIL) method for the diagnosis of blade cracks by measuring the real-time vibration of the wind turbine. However, this method was an indirect measurement, which was not able to measure vibration energy concentrated in the blade, such as in a blade–impeller system with a strong rotor stiffness.

The acquisition sensors are not in contact with test blades but are installed around the blades, which is called the non-contact vibration measurement method. This method, which is simple in structure and does not affect the original blade quality, stiffness, and other performance parameters, can detect the vibration state of all circled blades and has

gradually become a research focus in the field of blade vibration detection. Intermittent phase [6], laser holography [7], acoustic response [8], and blade tip timing [9] are some examples. Blade tip timing (BTT) technology is developed on the basis of the frequency modulation method. The arrival times of the blade to the displacement sensor mounted on the casing are recorded, and the vibration parameters of the blade can be obtained by analyzing the difference between the recorded times. BTT has the advantages of a simple structure and easy installation. It only needs to arrange the sensor in the casing to monitor the vibration status of all circled blades and does not affect the blades. Due to the sparsity of sampling, the BTT signal is severely undersampled, so it needs a recognition algorithm for data processing to further obtain the vibration parameters, which is also the main drawback of the blade tip timing technology.

In recent years, enterprises, research institutions, and universities have invested significant resources in the research of BTT technology in the field of turbomachinery, resulting in a wealth of research results and extensive experience in theoretical methods and engineering practice [10]. General Electric, Pratt &Whitney, and Rolls-Royce all applied BTT technology to the safety detection of engine blades [11]. At the Politecnico di Torino, the latest generation of BTT systems was used to identify the dynamic properties of rotating blade discs [12]. Madhavan et al. [13] adopted BTT to measure the abnormal vibration of an aeronautical gas turbine blade and applied it to detect blade damage. Hu et al. [14]. established the rotating integral blade disc detuning identification and model real-time calibration (BR-IDC) method based on BTT and achieved the online real-time detuning identification of rotating blade discs through experiments. Research on the acquisition of vibration parameters based on BTT signals has also been in progress. Imperial College proposed a sensor waveform analysis method based on BTT and clearance sensor waveform analysis methods (BLASMA) that can be used to determine single and multi-harmonic blade vibration parameters for asynchronous and synchronous vibrations [15]. Duan et al. [16] identified the blade arrival time using the rising and falling edges of the BTT signal and proposed a calibration procedure applicable to asymmetric BTT signals to improve the measurement accuracy. Lin et al. [17] proposed a multimodal blade vibration reconstruction algorithm to reconstruct the unknown multimodal blade vibration signal and also proposed a minimum requirement for the number of probes. Wang et al. [18] established an improved multi-signal classification (MUSIC) method to effectively identify the vibration frequency components in undersampled BTT signals.

The difficulty in analyzing blade fault signals stems not only from the fact that the blade fault is unpredictable and unknown but also from the fact that the early fault signal created during operation is latent. Fault diagnosis methods based on deep learning can efficiently analyze vast volumes of data, automatically extract data feature values, and generate correct diagnosis findings rapidly. The convolutional neural network (CNN) is one of the most successful deep learning approaches, employing local connections and shared weights to extract information features from data, while avoiding overfitting issues [19,20].

Research on blade fault diagnosis for undamped structures has gradually emerged recently. Gantasala et al. [21] proposed a method based on an artificial neural network (ANN) model to identify the location and quantity of ice mass on wind turbine blades, and this method correctly predicted the ice mass distribution along the blades. Joshuva et al. [22] applied machine learning to identify the impact of various blade failure circumstances on unit blades. Yu et al. [23] applied computational fluid dynamics and finite element analysis to numerically simulate the damage detection of single cracked blades and proposed an effective method to predict crack location and size based on the variation the natural frequency of wind turbine blades. Zhang et al. [24] proposed a method for detecting blade faults by fusing tip clearance information with BTT data, which was validated by 16 sets of experiments. The results showed that the classification accuracy reached 95%, which was significantly higher than traditional diagnostic methods. Wu et al. [25] used the k-means approach to classify faults in the BTT data of a titanium-bladed disk with cracks.

It is clear from the review above that BTT has attracted a lot of attention and research because it is currently the most effective technical method for detecting blade vibration [10]. Additionally, with the development of big data and artificial intelligence, deep learning-based detection methods have been successfully applied to the prediction of equipment faults. Due to this, the purpose of this research is to implement and enhance more effectively the application of intelligent diagnosis methods in blade fault vibration detection to improve blade fault diagnosis, as well as to extend the application of BTT in the field of blade fault diagnosis by using deep learning.

A fault diagnosis method for turbine blade cracks based on BTT and CNN is proposed in this research, which is validated in two ways: the numerical analysis of the intelligent diagnosis of rotating turbine blade cracks and the experimental examination of rotating blade crack fault diagnosis. The complete closed block diagram of the work is shown in Figure 1. The main contents mainly include:

(1) This research develops a numerical model of the concentrated parametric vibration of blades and a numerical model of the BTT signal acquisition. The measurement deviation and noise are also added to the BTT data. The blades with crack faults, crack locations, and crack depth under uniform speed conditions are diagnosed, and the study compares several machine learning approaches to confirm the detection accuracy of the proposed CNN fault diagnostic model.

(2) Rotating blade crack diagnosis tests based on BTT measurements are performed and validated using a finite element model. The blade crack position and depth are effectively detected under uniform speed conditions, supporting the proposed CNN fault diagnosis model even further.
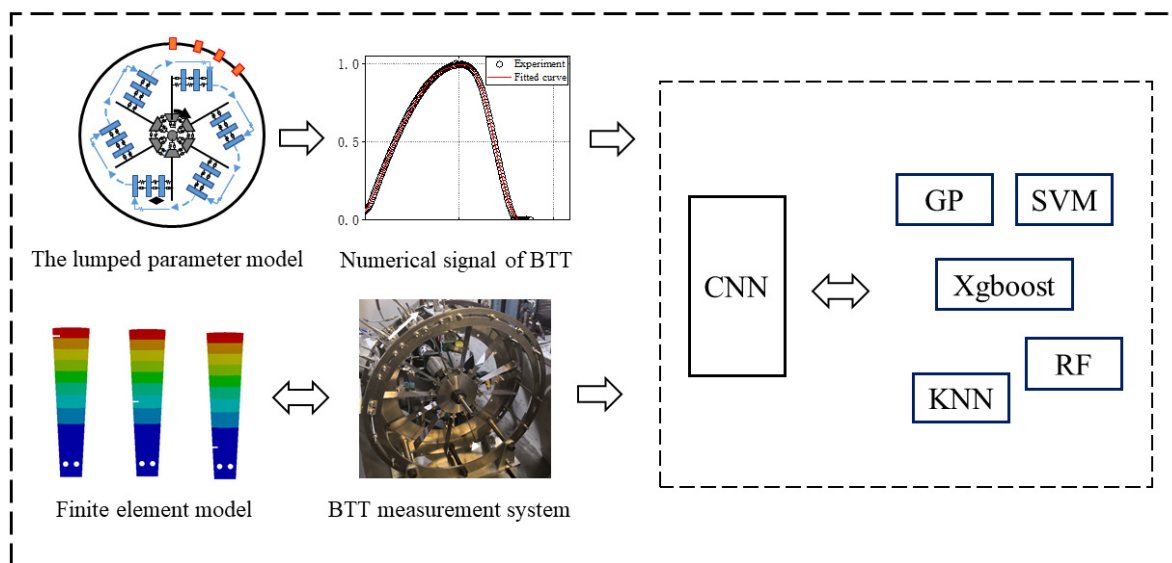


**Figure 1.** The complete closed block diagram.

The real-time monitoring of the blade vibration characteristics is required to reduce the risk of faults such as blade breakage and to increase blade vibration safety [10]. In this study, BTT is applied to determine the vibrational characteristics of cracked blades, and the CNN is used to automatically learn and extract fault signal features without relying on manual experience or signal analysis methods. This study gives a new perspective on fault detection in turbine blades and has great application potential for the intelligent health monitoring of blade discs. Additionally, it can be used to develop digital twin models [14] of blade discs and to predict the severity of blade cracks in real time.

## 2. Method

### 2.1. Numerical Model

The finite element model and the lumped parameter model are frequently used for the mathematical modeling of blades in scientific research or engineering analysis. The finite element model is based on real blade geometry. Therefore, the vibration analysis results are more detailed and accurate, but the computational time and resource consumption are very high. The lumped parameter model can only qualitatively describe the blade vibration characteristics. However, it can be programmed to analyze them quickly and provide a large and effective signal data set for failure vibration analysis.

A lumped parameter model for the combined cracked blade fault diagnosis problem is developed in this research, as shown in Figure 2. The whole circle blade model consists of 6 sectors, all of which are composed of 3 degrees of freedom, including the tip, body, and root of the blade, and 1 degree of freedom, including the rotor disk. The center of the rotor disk is connected to the rotor shaft to rotate the disk around the rotor shaft. The blade only vibrates in the direction of rotation. A dry friction-damping structure generates relative friction between the tips of adjacent blades based on their relative motion. The blades are modeled with 3 degrees of freedom in this work, which can demonstrate higher-order complex motion patterns in blade vibration. A total of four sensors are evenly distributed around the perimeter of the blades, with a 15° angle between them.
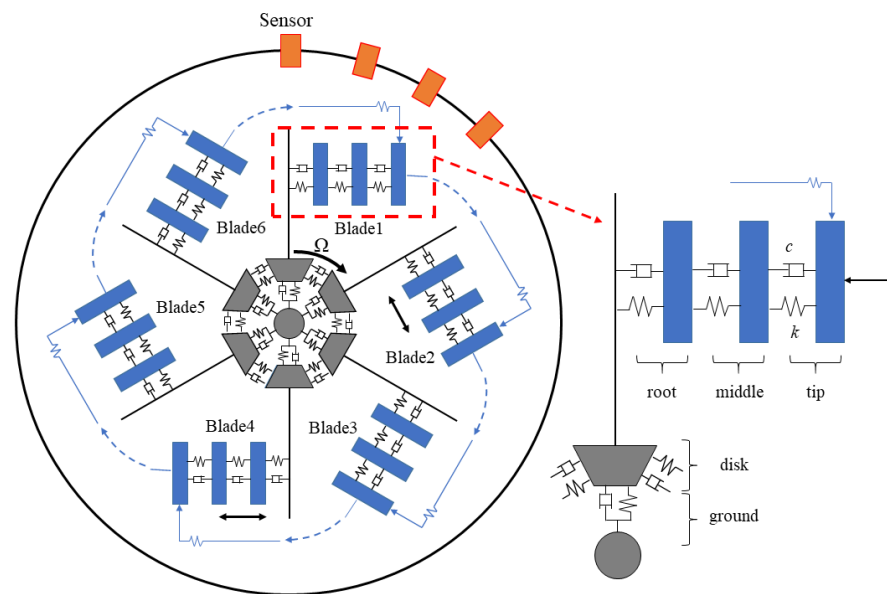


**Figure 2.** The lumped parameter model.

The lumped parameter model used in this study does not correspond to the experimental model because the lumped parameter model ignores a large number of real blade characteristics. Furthermore, in order to validate the method proposed in the study, the mutual influence factors between adjacent blades are added to the lumped parameter model, which is also different from the free blades used in the experiments.

The individual waveforms are separated from the sensor output based on the experimentally determined time-domain voltage signal and normalized to the original amplitude and pulse signal range according to the sensor probe size. As shown in Equation (1), the Fourier variation of the first four orders is retained to fit a waveform function of the relative distance between the blade and the sensor.

$$U(x_{i,j}) = a_0 + \sum_{i=1}^{n} a_i cos(i\omega x_{i,j}) + b_i sin(i\omega x_{i,j}) \tag{1}$$

where $x_{i,j}$ is the distance of the blade tip from the sensor center, $i$ is the order of the harmonic wave, $b_i$ is the angular frequency, $a_i$ is the cosine term coefficient, and $b_i$ is the sine term coefficient.

Cracks are assumed to appear at random in the top, middle, and root of blades in the numerical model, and the variation in cracks regarding stiffness values at different sites is defined as crack severity $\xi$. The stiffness value $k_{\mathrm{m}}$ at the location where the crack appears on the blade can be calculated by subtracting the crack severity $\xi$ from the harmonic value $k_{\mathrm{t}}$, as expressed by Equation (2):

$$k_{\mathrm{m}} = k_{\mathrm{t}}(1 - \xi) \tag{2}$$

The problem of blade fracture combinations is examined in this research, where cracks may be present in more than one blade. Cracks are added randomly to the top, middle, or root of a blade, and this detection task is a classification task. Blade crack severity is a continuous variable in the range [0, 0.5], with 0 indicating no cracks and the corresponding detection task is a regression task.

The system parameter deviation $y_{\mathrm{err}}$ and signal noise $u_{\mathrm{noise}}$ are added to the BTT voltage signals in this study to make the signals derived from the numerical model resemble the real blade signals more. The noise is 30 dB of white Gaussian noise.

The deviation of the system parameters affects the magnitude of the blade vibration displacement amplitude, and the signal noise affects the extraction of the blade tip arrival time. System parameter deviations $y_{\mathrm{err}}$ include structural deviation $y_{\mathrm{err}}^{\mathrm{b}}$, blade tip deformation under centrifugal force $\bar{y}_{\mathrm{err}}^{\mathrm{b}}(f_v(t))$, and sensor positioning deviation $\Delta y_{\mathrm{err}}^{\mathrm{s}}$, as in Equation (3):

$$y_{\mathrm{err}} = y_{\mathrm{err}}^{\mathrm{b}} + \bar{y}_{\mathrm{err}}^{\mathrm{b}}(f_v(t)) + \Delta y_{\mathrm{err}}^{\mathrm{s}} \tag{3}$$

In this study, it is assumed that the blade structure's structural deviation $y_{\mathrm{err}}^{\mathrm{b}}$ and sensor positioning deviation $\Delta y_{\mathrm{err}}^{\mathrm{s}}$ are random variables in the range of $[-0.5\ \mathrm{mm}, 0.5\ \mathrm{mm}]$; the blade tip deformation $\bar{y}_{\mathrm{err}}^{\mathrm{b}}(f_v(t)) = f_v(t)^2/10^5$, $f_v(t)$ is the rotation frequency.

The accurate extraction of the time of arrival from sensor signals is a fundamental requirement for performing research on BTT vibration measurement. The fixed voltage threshold method and the constant fraction crossing method are the two most commonly used methods. Due to the noise impact, these two methods often extract the incorrect BTT signal [26]. In order to obtain the signal accurately, this study proposes a BTT arrival time extraction method based on the linear fitting of the rising edge interval of the pulse voltage signal.

As shown in Figure 3, the signal's rising edge curve in the absence of noise is theoretically a continuous process with an approximately constant slope. This method selects a truncated voltage interval within an interval Ua ~ Ub containing the threshold voltage along the rising edge of the voltage signal curve, uses linear least squares fitting to obtain the rising curve, and then intersects with the threshold voltage level to solve for the intersection point corresponding to the time of arrival (TOA). The blade shape in Figure 3 is a schematic diagram of a generalized blade to illustrate how to obtain the blade tip arrival time and is not the blade shape used in the experiment.
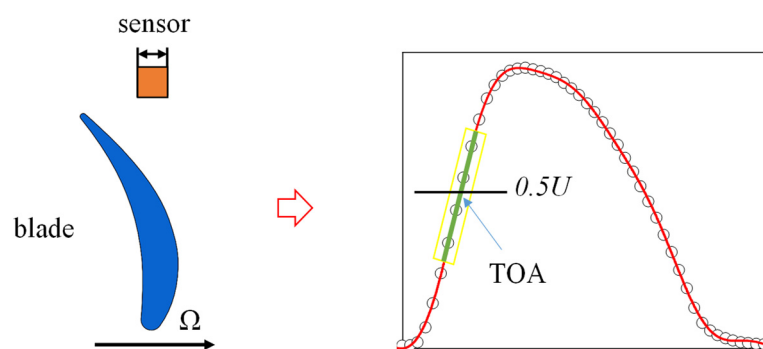


**Figure 3.** Method for obtaining blade tip arrival time.

### 2.2. CNN

A 1-D convolutional neural network (CNN) structure for blade crack fault detection is designed in this research, as shown in Figure 4. The vibration signal of cracked blades, obtained by numerical simulation or experimental test, is the input of the CNN network. The kernel size of the downsampling layer is 11, the step size is 4, and the kernel channel size is 64. In this research, a 5-layer 1-D convolutional network with a kernel size of 5 is adopted. Multiple layers of small convolutional kernels can make the network deeper, resulting in better feature representation and contributing to better network performance [27]. The last layer of the fully connected layer consists of two parts: the upper layer with output size 4 is used to output the crack location feature, and the lower layer with output size 1 is used to output the crack depth feature. The weights for the loss functions of the classification and regression tasks are adopted to generate the loss function of the total task. Adam is used in the optimizer, and the initial learning rate is set to 0.001. MSE and CrossEntropyLoss are adopted as cost functions to predict the value and type, respectively.
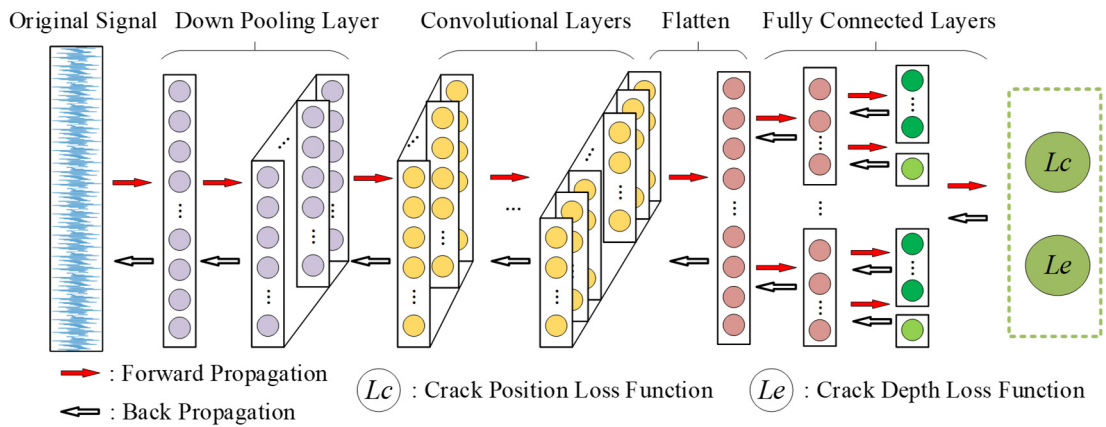


**Figure 4.** Convolutional neural network structure.

### 2.3. Testing Device

In this study, the blade vibration testing system based on BTT is devised to obtain vibration signal data from real cracked blades. The system components are shown in Figure 5. The test platform mainly consists of a rigid support cast iron platform, a servo motor, and bearing support.
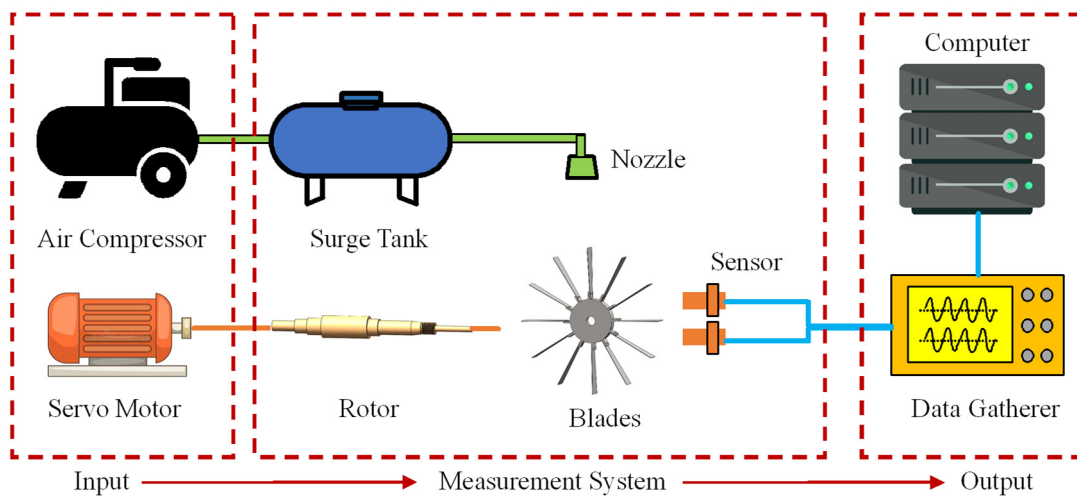


**Figure 5.** BTT test system structure.

The height dimension is much larger than the width and thickness dimensions for free blades with long and thin geometries, such as compressor first-stage blades, fan blades, and turbine final-stage blades. In this study, to improve signal collectability and reduce the influence of noise, a simplified trapezoidal flat blade with a long and thin geometry is designed. In addition, the method can be extended to applications with characteristics similar to the blade design in this research, such as the compressor's first-stage blade. The test blade is loaded in two ways: first, by centrifugal force in the rotating state, and second, by an airflow excitation force applied to the top position of the blade to cause vibration, which is also similar to the real blade loading conditions. The blade damage form in this research only includes crack failure, which has two characteristics: location and depth.

Straight blades are used for the test. The thickness of the blades is 1.2 mm, and the length is 120 mm. Cracks in this test are designed at three locations, including the top, middle, and root of the blade. The maximum machining depth of the blade crack is 30% of the depth of the section where the crack is located. The test speed is 1500 rpm.

The test object of this study is a full-circle model blade with a blade thickness of 1.2 mm and a blade length of 120 mm. The specific blade material and geometric parameters are shown in Table 1.

**Table 1.** Material and geometric parameters of the blade.

| Project | Parameter |
|---|---|
| Material | ASTM 1045 |
| Number of blades | 12 |
| Disc diameter/mm | 120 |
| Height of blade/mm | 138 |
| Height of the bottom of the blade/mm | 62 |
| Top length/mm | 34.4 |
| Bottom length/mm | 20 |
| Thickness of blade/mm | 1.2 |

Figure 6 shows the installation position of the blade, the shape parameters of the blade, and the cracks in the root position.
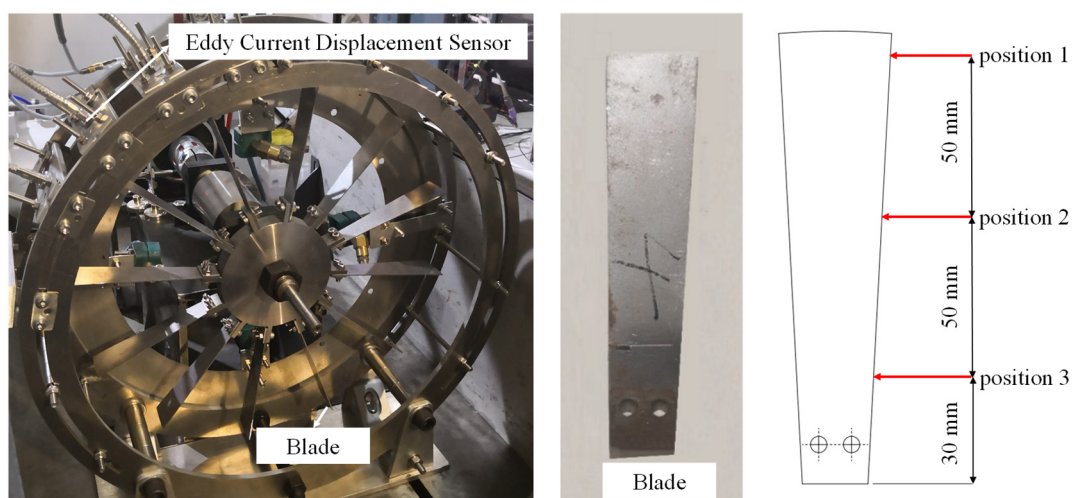


(**a**) Test blades　　　　　　　　　　　　　　　　(**b**) Cracked blades and crack locations

**Figure 6.** Test blades and crack locations.

The objective of this test is to detect the crack location and crack depth of the blade based on the BTT signal obtained from the cracked blade test. The vibration signal acquisition is affected by random errors such as sampling frequency, system device installation deviation, and noise.

The number of BTT data with random crack depths obtained for each crack location in the testing is set to 30, while one set of crack-free conditions is added for comparison. The test duration of each group is 90 s, and the data volume of the fault diagnosis input signal is increased 10 times by further averaging each group of test data into 10 segments of data samples.

## 3. Results

### 3.1. Results of Lumped Parameter Model

3.1.1. Comparison of Results of Fault Diagnosis Models

In order to verify the effectiveness of the fault diagnosis model in this paper, Gaussian Process (GP), Support Vector Machines (SVMs), eXtreme Gradient Boosting (Xgboost), K-Nearest Neighbor (KNN), Random Forests (RFs) are compared with the CNN model proposed in this paper.

A total of four different cases are designed for the fault detection task based on whether system deviation and noise are factored in (conditions for system deviation and noise are described in Section 2.1). Figure 7 shows the accuracy results of the CNN model in this paper and five other machine learning algorithms for blade crack location detection. Compared with the other five machine learning models, the CNN model achieves the highest level of prediction accuracy in four cases: 91.7%, 88.0%, 91.1%, and 86.7%, respectively. The prediction accuracy of the other five machine learning models is significantly reduced, especially under complex conditions with system deviation and noise, while the CNN model in this paper still performs well.
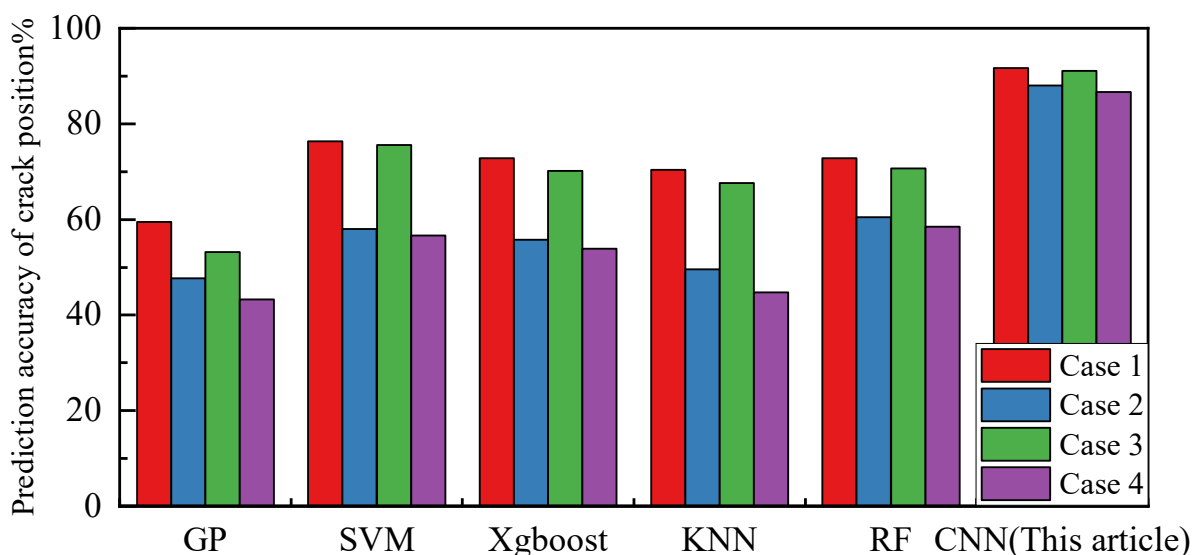


**Figure 7.** Prediction accuracy of blade crack location by different deep learning models (case 1: No system deviation and No noise; case 2: System deviation and No noise; case 3: Noise and No system deviation; case 4: System deviation and Noise).

Figure 8 shows the accuracy results of the CNN and five other machine learning methods for blade crack depth prediction. Similarly, in four cases, the CNN model developed in this study outperforms the other five models in predicting blade crack depth by 95.4%, 90.7%, 94.6%, and 87.5%, respectively.
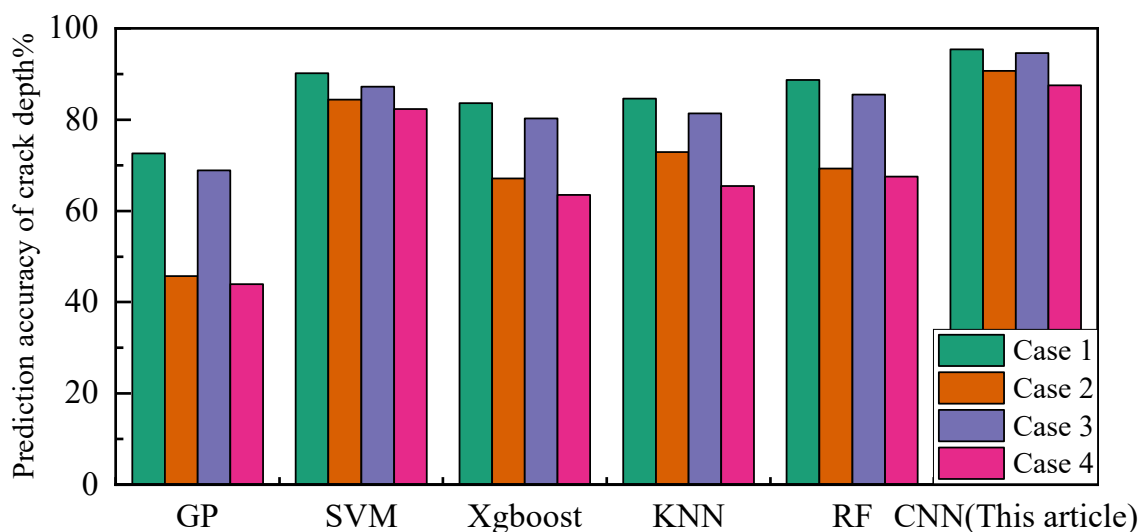
**Figure 8.** Prediction accuracy of blade crack depth by different deep learning models (case 1: No system deviation and No noise; case 2: System deviation and No noise; case 3: Noise and No system deviation; case 4: System deviation and Noise).

Through comparison, the CNN model proposed in this research is better than the traditional machine learning model in multiple ways. The traditional machine learning model typically can only utilize a single task detection problem, whereas the CNN model can utilize a multi-task problem of crack location and depth at the same time. The detection accuracy of the CNN model established in this paper is significantly higher than that of the five different traditional machine learning models, and the CNN model shows stronger adaptability under system deviation and noisy working conditions.

3.1.2. Prediction of Blade Crack Location and Depth

This section shows the fault diagnosis results obtained by the CNN method in this study for four cases in terms of crack location and depth. The confusion matrix of the blade crack location detection results is depicted in Figure 9. Positions 0 to 3 indicate no crack, top cracks, mid cracks, and root cracks, respectively. In addition, the values in the matrix reflect the proportion of correct detections in the true value to the total number of results in that category. As shown in Figure 9, the classification of crack faults is weak for locations 2 and 3; locations 0 and 1 are better, and the classification results are more than 80% for each case. The results show that the CNN is very effective at this task. However, many crack faults are not diagnosed as cracks, since the crack fault characteristics are imparted upon the no-crack blades during the coupling action, leading to confusion in the diagnostic identification. It is evident from a comparison of Figure 9a–c that deviations have a stronger influence on crack fault prediction, particularly for the prediction of no cracks. Since noise has less impact on the identification method than systematic deviation does, system deviation directly affects the identification of blade vibration characteristics.

Figure 10 shows the blade crack depth prediction results for four different cases. It can be seen that the detection results in Figure 10a,c are relatively stable throughout the whole change in crack severity, and the errors are mostly within 10%, while the detection results in Figure 10b,d have larger errors between the predicted and real values due to system deviation and noise. The prediction accuracies are calculated to be 95.4%, 90.7%, 94.6%, and 87.5% for the four cases, respectively. Comparing Figure 10a–c, the noise has less impact on the prediction of blade crack depth. It is clear that the system deviation causes the data to have a more discrete distribution, increasing the error between the predicted and true values. The reason is that the system deviation directly affects the results of the BTT signal recognition.
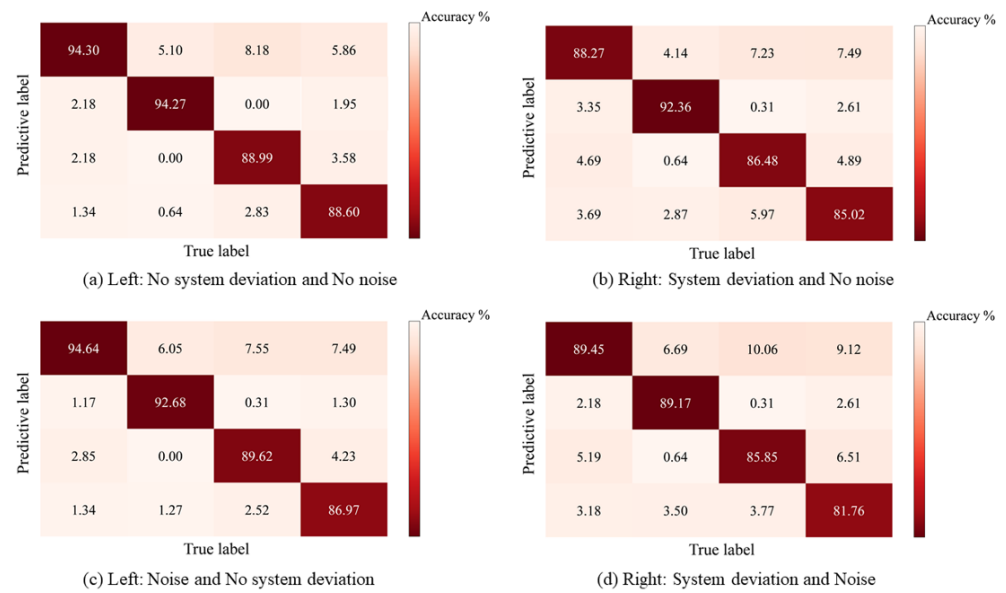
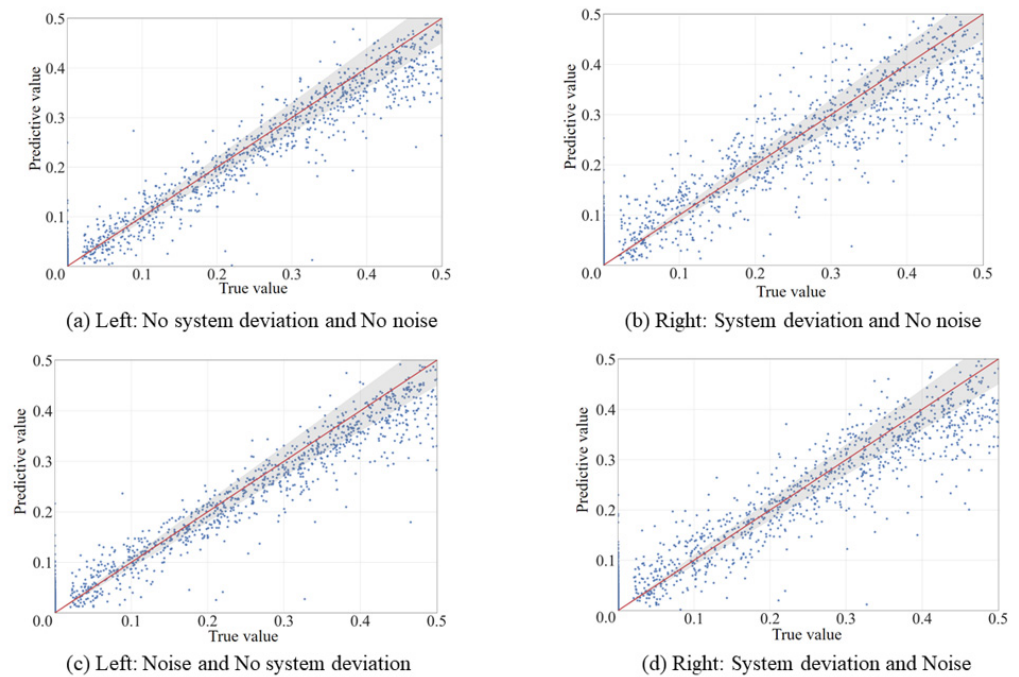**Figure 9.** Confusion matrix of blade crack location detection results.



**Figure 10.** Regression curve of blade crack degree detection results.

*3.2. Results of Experimental Measurement Data*

3.2.1. Analysis of Blade Fault Vibration Characteristics

A finite element numerical analysis is adopted to obtain the blade modal and response characteristics under various crack location and crack depth conditions. From the numerical analysis results, the key characteristic parameters for fault identification can be obtained to guide the experimental design. In this study, the numerical model is verified by the variable speed sweep method.

The Campbell diagram of blade vibration and the modal vibration patterns for the first three orders of vibration are given in Figure 11. The result shows that the first-order resonance of the blade may occur between 500 rpm and 1500 rpm for integer multiples of the speed, with resonance points of 611.4 rpm, 739.9 rpm, 936.9 rpm, and 1292.0 rpm for

the line of excitation from three to six, corresponding to vibration frequencies of 61.14 Hz, 61.66 Hz, 62.46 Hz, and 64.60 Hz.
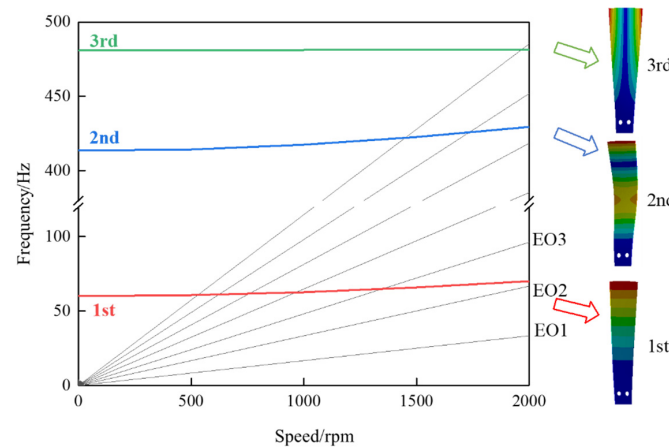


**Figure 11.** Campbell diagram of modal frequency of model blade.

The test speed is set to rise from 0 rpm to 1600 rpm with a uniform acceleration for 96 s and a maximum speed frequency of 26.67 Hz. As shown in Figure 12, the Campbell diagram of blade vibration is obtained using wavelet analysis based on the measured strain gauge's time-domain signal. It can be seen that the blade resonates at multiple multiples in the speed range.
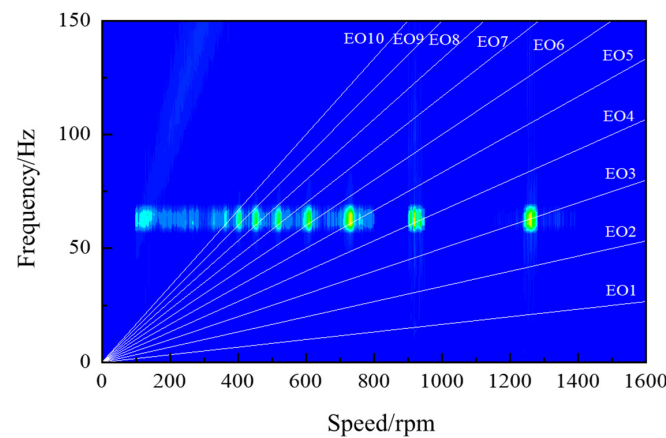


**Figure 12.** Campbell diagram of variable speed strain signal based on wavelet analysis.

Table 2 gives the results of the measured intrinsic frequencies of the strain gauges at each octave, which is very close to the numerical analysis results, with a maximum error of 2.8% for the numerical analysis of the blade vibration frequencies.

**Table 2.** Experimental and numerical analysis of blade vibration frequency results at each octave.

| Frequency Multiplication | 3 | 4 | 5 | 6 |
|:---:|:---:|:---:|:---:|:---:|
| Numerical prediction/Hz | 64.60 | 62.46 | 61.66 | 61.14 |
| Experimental measurement/Hz | 62.84 | 62.49 | 61.04 | 60.83 |
| Numerical error/% | 2.80 | −0.05 | 1.02 | 0.51 |

In the numerical model, the natural frequencies at nine uniform depths from 1/30 to 9/30 were analyzed at each crack depth, considering the crack locations at the top of the blade, the middle of the blade, and the root of the blade, respectively.

Figure 13 shows the variation curve of the natural frequency of the cracked blade's first, second, and third-order vibration modes with crack depth. When the crack is in the middle and root positions of the blade, the modal frequency decreases as the crack depth increases. In addition, when the crack is in the top position, the blade modal frequency slightly increases as the crack depth increases. The reason is that the influence of the actual blade crack processing mode reduces the quality of the blade tip position. According to the results, the natural frequency of the blade can be applied as a sensitive parameter to indicate the condition of the blade crack. In the same crack depth case, the blade modal frequency is more sensitive to cracks appearing at the root of the blade.
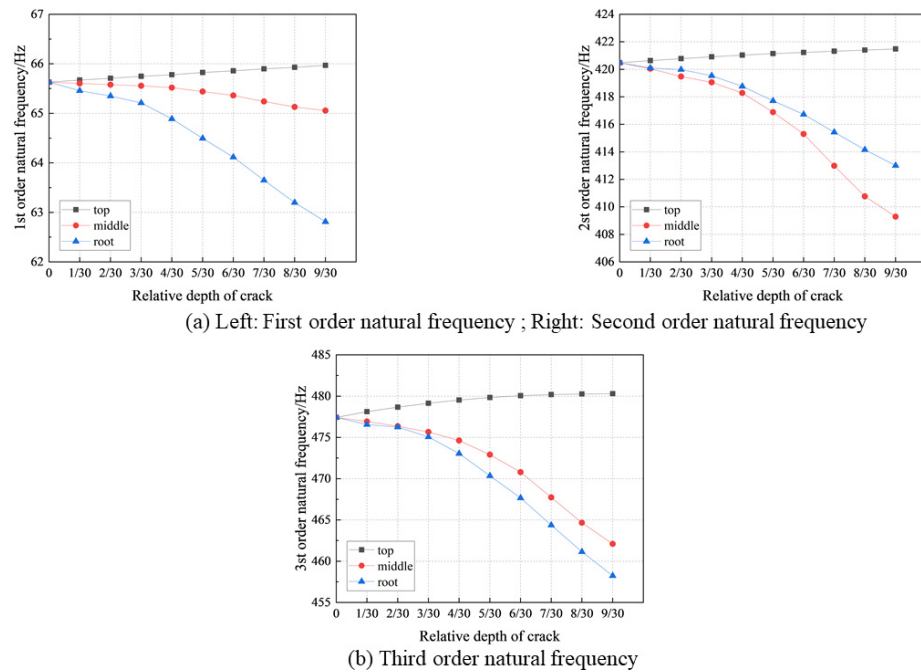


(a) Left: First order natural frequency ; Right: Second order natural frequency



(b) Third order natural frequency

**Figure 13.** The first three orders of natural frequency of the blade at different crack depths.

### 3.2.2. Results Comparison of Different Fault Diagnosis Models

Similarly, this paper compares the performance based on experimental data of SVM, Xgboost, KNN, RF models, and CNN. Figure 14 shows the results of the prediction accuracy of crack location and crack depth. The maximum accuracy of traditional machine learning methods for crack location and depth detection is 85.7% and 66.3%, respectively, while the prediction accuracy of the CNN is 91.6% and 88.2%. Compared to several other machine learning models, the CNN designed in this study has better accuracy in detecting blade crack location and crack depth.
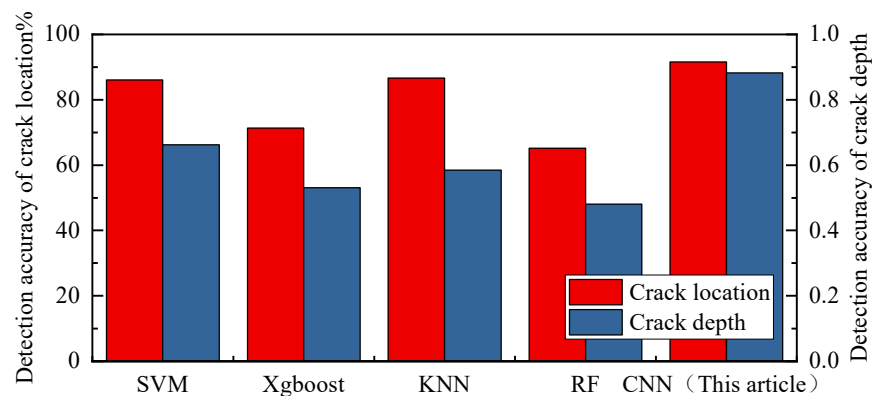


**Figure 14.** Prediction accuracy of different deep learning models.

The confusion matrix of crack location classification for the test set is shown in Figure 15a. Furthermore, the classification accuracy for the blade crack failure location is high. Only part of location one (the crack in the top) is incorrectly predicted as a crack in other locations, which also contributes to its relatively low prediction accuracy. The main reason may be the small effect of crack position one on blade frequency and the small difference in vibration amplitude of the cracked blade, which also corresponds to the results in Figure 13. Figure 15b shows the density statistics of the relative errors in the test results. The bar graph represents the density of distribution within each error interval, and the curve represents the Gaussian distribution of relative errors. When the width of the curve is smaller and the centerline is closer to 0, it indicates that the predicted results are more accurate. From the figure, it can be seen that the error of most of the predicted values of the crack degree is within ±20%.
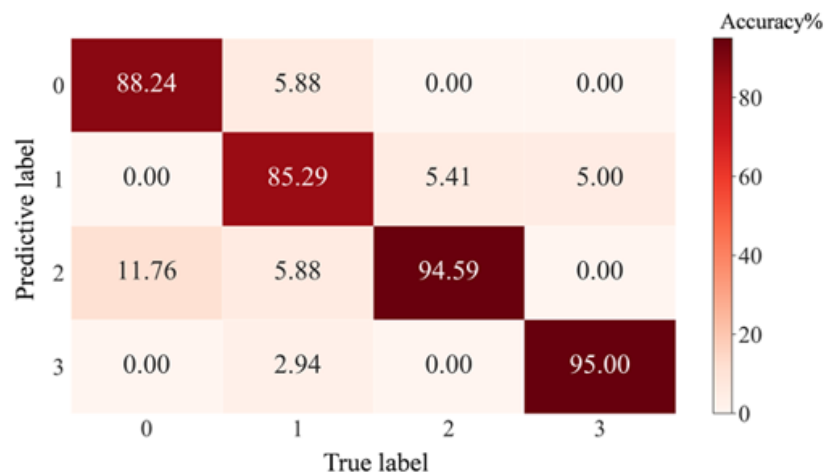


(a) Confusion matrix
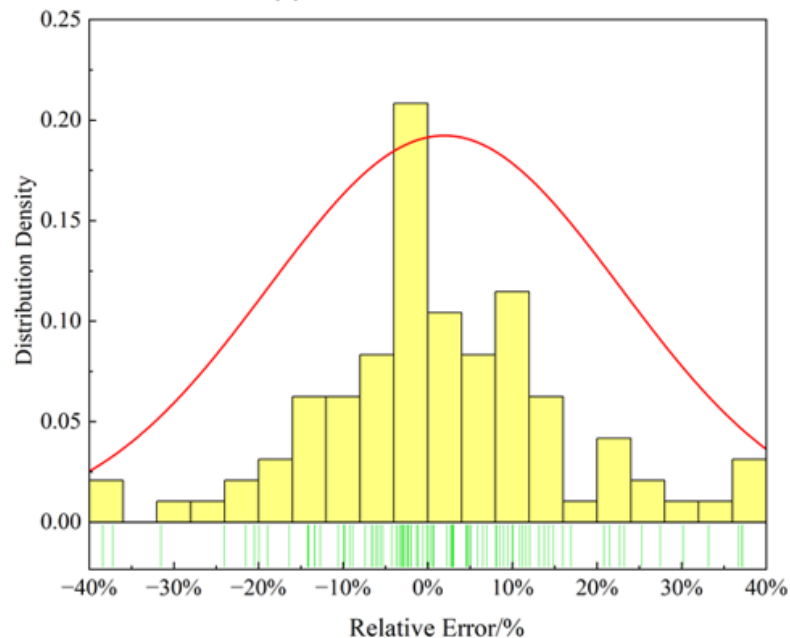


(b) The density statistics of Regression Error

**Figure 15.** Detection results of crack location and depth of 1500 rpm blade.

## 4. Conclusions and Forecast

A CNN-based blade crack detection and analysis method is proposed to improve the low accuracy of blade fault diagnosis in rotating turbine blade vibration. Fault signal

features can be automatically extracted and learned, and the high workload and uncertainty of traditional manual extraction are eliminated. Secondly, the numerical analysis of blade crack vibration measurement based on BTT is carried out. The numerical model of the sensor output voltage signal is established, and the effectiveness of the CNN fault diagnosis model in predicting the blade crack location and extent under the conditions of simulating the actual measurement deviation and noise is verified. The results show that the proposed CNN model can be applied to the complex problem of crack fault detection in untuned turbine blades. Finally, the vibration measurement of the rotating blade crack faults based on BTT is studied, and the results verify the effectiveness of the proposed CNN fault diagnosis model for the intelligent diagnosis of blade crack location and depth. The summarized conclusions are as follows.

(1) A fault diagnosis method for blade cracks based on convolutional neural networks has been developed. This method detects blade crack faults by deeply mining the data features of the input signal, and this method is anti-interference and noise-resistant.

(2) The accuracy of traditional machine learning models such as GP, KNN, RFs, SVMs, and XGBoost for cracked blades is much lower than that of the CNN model proposed in this paper. Moreover, traditional machine learning models perform poorly in deviation conditions and are difficult to adapt to the actual complex testing environment.

(3) Based on the proposed CNN crack detection model, a crack detection analysis for the rotating blade tip timing numerical model with cracks is constructed. The results show that the crack fault can be effectively identified by this method considering system deviation and signal noise. For the given four cases, the prediction accuracy of crack location is 92.9%, 87.7%, 90.8%, and 85.8%, respectively, while the prediction accuracy of crack depth is 95.4%, 90.7%, 94.6%, and 87.5%.

(4) The effectiveness of the CNN fault diagnosis analysis model has been verified by rotating blade crack detection test BTT data. The method can effectively detect the crack location and depth condition. The detection accuracy of the crack location is 91.6%, and the detection accuracy of the crack depth is 88.2%, which has a higher diagnosis level compared to the other machine learning models.

Vibration stress is an important parameter for the reliability of turbine blades. In subsequent research, the research on vibration stress detection of rotating blades based on the blade tip timing system will be developed to realize the inversion of the vibration stress of actual cracked turbine blades and to establish a blade safety monitoring method based on dynamic stress.

**Author Contributions:** Conceptualization, G.Z. and C.W.; methodology, G.Z. and C.W.; software, D.G.; validation, G.Z., W.Z. and D.G.; formal analysis, G.Z.; investigation, C.W.; re-sources, W.Z.; data curation, W.Z.; writing—original draft preparation, G.Z.; writing—review and editing, D.G. and C.W.; visualization, W.Z.; supervision, Y.X.; project administration, D.Z.; funding acquisition, Y.X. and D.Z. All authors have read and agreed to the published version of the manuscript.

**Institutional Review Board Statement:** Not applicable.

**Informed Consent Statement:** Not applicable.

**Data Availability Statement:** Data is unavailable due to privacy.

**Conflicts of Interest:** The authors declare no potential conflict of interest with respect to the research, authorship, and/or publication of this article.

## References

1.  El-Bayoumy, L.E.; Srinivasan, A.V. Influence of Mistuning on Rotor-Blade Vibrations. *AIAA J.* **1975**, *13*, 460–464. [CrossRef]
2.  Gui, Z.Y. *Research on the Key Technology of Non-Contact Online Monitoring of Flue Gas Turbine Blade Vibration*; Tianjin University: Tianjin, China, 2008. (In Chinese)
3.  Spitas, V.; Spitas, C.; Michelis, P. A three-point electrical potential difference method for in situ monitoring of propagating mixed-mode cracks at high temperature. *Measurement* **2010**, *43*, 950–959. [CrossRef]
4.  Krause, T.; Ostermann, J. Damage detection for wind turbine rotor blades using airborne sound. *Struct. Control. Health Monit.* **2020**, *27*, e2520. [CrossRef]
5.  Abouhnik, A.; Albarbar, A. Wind turbine blades condition assessment based on vibration measurements and the level of an empirically decomposed feature. *Energy Convers. Manag.* **2012**, *64*, 606–613. [CrossRef]
6.  Leon, R.L.; Trainor, K. Monitoring systems for steam turbine blade faults. *Pollutants* **1990**, *24*, 12–15.
7.  Sikora, J.P.; Mendenhall, F.T. Holographic vibration study of a rotating propeller blade. *Exp. Mech.* **1974**, *14*, 230–232. [CrossRef]
8.  Yan, W.; Wen, G.D. Test on acoustic vibration fatigue characteristics of aeroengine rotor blades. *J. Aerosp. Power* **2016**, *31*, 2738–2743. (In Chinese)
9.  Heath, S.; Imregun, M. An improved single-parameter tip-timing method for turbomachinery blade vibration measurements using optical laser probes. *Int. J. Mech. Sci.* **1996**, *38*, 1047–1058. [CrossRef]
10. Rzadkowski, R.; Kubitz, L.; Maziarz, M.; Troka, P.; Dominiczak, K.; Szczepanik, R. Tip-Timing Measurements and Numerical Analysis of Last-Stage Steam Turbine Mistuned Bladed Disc During Run-Down. *J. Vib. Eng. Technol.* **2019**, *8*, 409–415. [CrossRef]
11. Ping, W. Application of tip timing method in foreign aeroengine blade vibration measurement. *Aeronaut. Sci. Technol.* **2013**, 5–9. (In Chinese) [CrossRef]
12. Battiato, G.; Firrone, C.M.; Berruti, T.M. Forced response of rotating bladed disks: Blade Tip-Timing measurements. *Mech. Syst. Signal Process.* **2017**, *85*, 912–926. [CrossRef]
13. Madhavan, S.; Jain, R.; Sujatha, C.; Sekhar, A. Vibration based damage detection of rotor blades in a gas turbine engine. *Eng. Fail. Anal.* **2014**, *46*, 26–39. [CrossRef]
14. Hu, D.; Wang, W.; Zhang, X.; Chen, K. On-line real-time mistuning identification and model calibration method for rotating blisks based on blade tip timing (BTT). *Mech. Syst. Signal Process.* **2020**, *147*, 107074. [CrossRef]
15. Heller, D.; Sever, I.; Schwingshackl, C. A method for multi-harmonic vibration analysis of turbomachinery blades using Blade Tip-Timing and clearance sensor waveforms and optimization techniques. *Mech. Syst. Signal Process.* **2020**, *142*, 106741. [CrossRef]
16. Duan, F.; Zhang, J.; Jiang, J.; Guo, H.; Ye, D. Method to improve the blade tip-timing accuracy of fiber bundle sensor under varying tip clearance. *Opt. Eng.* **2016**, *55*, 14106. [CrossRef]
17. Lin, J.; Hu, Z.; Chen, Z.-S.; Yang, Y.-M.; Xu, H.-L. Sparse reconstruction of blade tip-timing signals for multi-mode blade vibration monitoring. *Mech. Syst. Signal Process.* **2016**, *81*, 250–258. [CrossRef]
18. Wang, Z.; Yang, Z.; Wu, S.; Li, H.; Tian, S.; Chen, X. An Improved Multiple Signal Classification for Nonuniform Sampling in Blade Tip Timing. *IEEE Trans. Instrum. Meas.* **2020**, *69*, 7941–7952. [CrossRef]
19. Krizhevsky, A.; Sutskever, I.; Hinton, G.E. Imagenet classification with deep convolutional neural networks. *Commun. ACM* **2017**, *60*, 84–90. [CrossRef]
20. Esteva, A.; Kuprel, B.; Novoa, R.A.; Ko, J.; Swetter, S.M.; Blau, H.M.; Thrun, S. Dermatologist-level classification of skin cancer with deep neural networks. *Nature* **2017**, *542*, 115–118. [CrossRef]
21. Sudhakar, G.; Jean-Claude, L.; Jan-Olov, A. Investigating how an artificial neural network model can be used to detect added mass on a non-rotating beam using its natural frequencies: A possible application for wind turbine blade ice detection. *Energies* **2017**, *10*, 184.
22. Joshuva, A.; Sugumaran, V. A lazy learning approach for condition monitoring of wind turbine blade using vibration signals and histogram features. *Measurement* **2019**, *152*, 107295. [CrossRef]
23. Yu, M.; Fu, S.; Gao, Y.; Zheng, H.; Xu, Y. Crack Detection of Fan Blade Based on Natural Frequencies. *Int. J. Rotating Mach.* **2018**, *2018*, 2095385. [CrossRef]
24. Zhang, J.-W.; Zhang, L.-B.; Duan, L.-X. A Blade Defect Diagnosis Method by Fusing Blade Tip Timing and Tip Clearance Information. *Sensors* **2018**, *18*, 2166. [CrossRef] [PubMed]
25. Wu, S.; Wang, Z.; Li, H.; Yang, Z.; Chen, X. Blade Crack Detection Using Blade Tip Timing. *IEEE Trans. Instrum. Meas.* **2021**, *70*, 1–3. [CrossRef]
26. Diamond, D.; Heyns, P.; Oberholster, A. Constant speed tip deflection determination using the instantaneous phase of blade tip timing data. *Mech. Syst. Signal Process.* **2020**, *150*, 107151. [CrossRef]
27. He, K.; Zhang, X.; Ren, S.; Sun, J. Deep residual learning for image recognition. In Proceedings of the IEEE Computer Society Conference on Computer Vision and Pattern Recognition (CVPR), Las Vegas, NV, USA, 27–30 June 2016; pp. 770–778. [CrossRef]